ELSEVIER

Tribology International 35 (2002) 245–254

TRIBOLOGY INTERNATIONAL

www.elsevier.com/locate/triboint

Measurements of friction-induced surface strains in a steel/polymer contact

B.J. Briscoe [a], A. Chateauminois [b,*]

[a] *Particle Technology Group, Department of Chemical Engineering, Imperial College of Science, Technology and Medicine, Prince Consort Road, London SW7 2BY, UK*

[b] *Ecoles Supérieure de Physique et Chimie Industrielles (ESPCI), Laboratoire PCSM, UMR 7615, 10 rue Vauquelin, 75231 Paris Cedex 5, France*

Received 23 January 2001; received in revised form 4 December 2001; accepted 11 December 2001

Abstract

The paper describes an experimental study combined with analyses and numerical simulations of the surface strains developed in a metal–polymer contact under a variety of loading configurations. Specifically, a steel ball is caused to slide over a poly(methylmethacrylate) flat counterface under a fixed normal load where the imposed motions are small and consist of sliding and rotation and the combination of both. The surface strains have been measured directly using conventional strain gauges in two types of configurations specifically designed to monitor the strains for sliding and rotation. Calculations of frictional forces provide friction coefficients which are self-consistent and the computed 'friction displacement loops' correspond closely to those measured. In addition, the surface strain measurements provide a convenient and accurate insight into the stick–slip transitions in fretting contacts.

Keywords: Friction measurement; Fretting; Polymer

1. Introduction

The measurement of interfacial frictional forces has a very long history [1] and in recent periods has rather focused upon the application of 'force transducers', perhaps mainly because of the desire to retrieve continuous data with an electronic signature. Most transducers of practical value operate by relating a displacement, often small, to the imposed frictional force; the classical Eldredge and Tabor [2] and the Bowden and Leben [3] machines operated in this way. More recent and 'stiffer' transducers have been extensively used in areas where transducer compliance is a major constraint upon the practicability of the experiments; this is a major concern in fretting studies where the imposed displacements are of the same order of magnitude as the mechanical relaxation of the transducer arrangement. Similarly there are many cases where the dynamics of the transducer have been shown to have a major influence upon the sensed frictional behaviour [4,5]. The problem has been a significant issue in the interpretation of the origins of stick–slip and discontinuous sliding behaviour. Some experimentalists have found ways of using the frictional couple to access frictional forces without the use of a deliberate transducer arrangement [6,7]. In any event, it is now well appreciated that the perceived frictional response is a complex function of the interactions between the contact behaviour, the substrates, the machine and, when incorporated, the force transducers. As a simple matter of principle, one would try to reduce the number of complicated components in the frictional examination in order to provide an unequivocal description of the true interfacial friction response. The present paper examines the use of strain gauge elements, deposited upon the surface of one of the contacting member, as a mean to quantify the friction behaviour. The use of such gauges in routine stress/strain measurements during mechanical testing is well mastered and is common practice. The application in the context of friction measurements is thus common and the paper examines the value of this approach for a fretting contact generated between a steel and a polymer

* Corresponding author. Tel.: +33-1-40-79-47-87; fax: +33-1-40-79-46-86, http://www.umr7615.espci.fr/~chateau/index.html.

E-mail address: antoine.chateauminois@espci.fr (A. Chateauminois).

0301-679X/01/$ - see front matter
PII: S0301-679X(02)00002-6

Nomenclature

a	Radius of the Hertzian contact area
c	Radius of the central stuck area non-dimensionalised with respect to the radius, a, of the contact area.
E	Young's modulus
$E(x)$	Complete elliptic integral of the second kind
$f(x)$, $g(x)$	functions of the space coordinate x
G	Shear modulus
$K(x)$	Complete elliptic integral of the first kind
P	Normal load
p_0	Maximum Hertzian pressure
Q	Tangential load
θ	Angle of rotation of the steel ball
μ	Coefficient of friction
ν	Poisson's ratio

counterfaces. In the current paper, the strain gauges were located on the low modulus polymeric material in order to measure strains which are large enough to be detected using conventional gauges and their associated conditioning and processing apparatus. Two main contact loading conditions, involving oscillating sliding motions, have been considered for a typical fretting experiment: in the first one a steel ball was periodically twisted against a polymer flat, while in the second configuration, the ball was rotated about an axis parallel to the polymer body. For both configurations, the contact area presented the advantage of being stationary with respect to the location of the strain gauges. This contact loading condition simplified the processing of the time-dependent gauge output, which was then only related to the time-dependence of the imposed loading and not to changes in the location of the contact area with respect to that of the gauges.

In addition, complex contact conditions involving the combination, to various extents, of torsional and linear sliding motions have also been considered in order to evaluate the potential of such strain gauges measurements, under a complex contact loading, as a mean to quantify the friction behaviour. The strain gauges measurements to be reported were directed toward providing two basic types of information:

(i) The values of the coefficient of friction under the various contact loading configurations. The latter have been calculated from the measured surface strains by means of a now classical theoretical contact mechanical analysis.
(ii) The ability of the technique to determine the nature of the local contact conditions under the action of small amplitude tangential motions, i.e. fretting. Under such tribological conditions, it is well established that the occurrence of the main damage induced is largely governed by the complex distributions of the induced micro-motions within the contact zone [8]. For a ball-on-flat configuration, i.e. a circular contact area, it has been demonstrated [9,10] that the application of a tangential force induces micro-slip in an outer annulus surrounding the central part of the contact area where no slip occurs. When the tangential force is increased, the radius of the inner region of non-slip domain decreases until gross sliding conditions are reached within the whole contact area. Experimental investigations have established that the knowledge of the critical transition between these so-called partial slip and gross slip conditions is of primary importance in order to predict whether the primary initial damage mechanisms will be related to either wear processes or to contact cracking when the contact parameters are varied [11]. In the present study, an attempt was therefore made to identify this transition from the measurement of the surface strain as a function of the imposed displacement.

2. Experimental and numerical details

2.1. Materials and friction device

The fretting experiments were designed in order to investigate contact conditions involving various extents of, and combinations of, linear and torsional sliding motions. These complex contact zone kinematics were generated in a contact between a poly-(methylmethacrylate) (PMMA) flat and a steel ball which was submitted to small amplitude rotating motions. By varying the angle, α, between the axis of rotation of the ball and the surface of the PMMA speci-

men, it was possible to combine the rotational and linear sliding motions within the contact; Fig. 1(a). In the present study, α ranged from 0° (torsional contact conditions) to 90° (linear sliding conditions). The fretting device used has already been described in details elsewhere [12,13]. It consisted of a free lever arm with the flat PMMA specimen attached to one side (Fig. 1(b)). Dead weights were used to load the PMMA specimen into contact with the steel ball, which was attached to a rotary stage by means of a shaft. An oscillating rotation at constant angular velocity (2°/s) was imposed to the stage by means of a reduction-geared stepper motor controlled by computer software. For all the experiments to be described, the normal load was set to 20 N. The diameter of the resulting Hertzian nominal contact area was 730 μm, with a mean contact pressure of 48 MPa (the modulus of the PMMA was taken as 3.5 GPa, the Poisson's ratio as 0.35). Depending on the loading configuration, the magnitude of the imposed angular motion varied from 0.3 to 5° in order to investigate contact conditions ranging from partial slip to gross slip. During the fretting process, the imposed angle of twist, θ, was continuously monitored by means of a LVDT transducer attached to the ball drive shaft; Fig. 1(b).

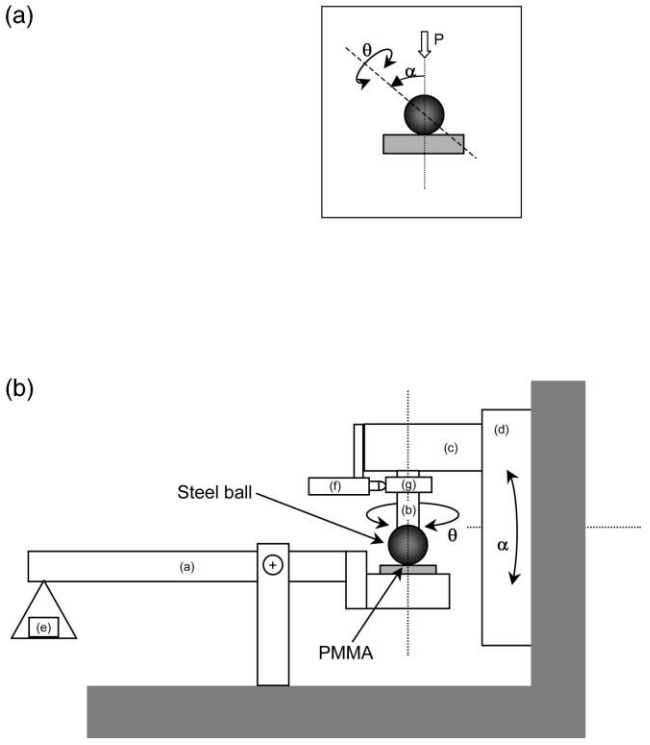

Fig. 1. Schematic description of the fretting device. (**a**) Description of the contact loading parameters. P is the applied normal load, α is the angle between the axis of rotation of the ball and the surface of the PMMA specimen, θ is the angle of twist of the ball. (**b**) Side view of the fretting rig. (a) pivoted lever arm; (b) ball driving shaft; (c) rotary stage and stepper motor system; (d) vertical rotary stage; (e) dead weights; (f) LVDT transducer; (g) moving plate attached to the ball driving shaft. The LVDT transducer is used to measure the angular displacement of the steel ball from the displacement of the moving plate (g) when the drive shaft (b) is rotating.

The PMMA system was a commercial grade of cast Perspex® (ICI Acrylics, UK). Flat specimens (15×60 mm) of ca. 5 mm thickness were washed in a neutral aqueous detergent solution (Neutracon®) prior to use. The steel counterface was an ASI 52100 standard bearing ball with a radius of 12.65 mm. Before use, the steel ball was cleaned using 'Analar' ethanol.

120 ohms strain gauges with a polyimide backing were used in all the experiments (manufactured by TLM, Japan). Their transverse sensitivity factor was 0.7%. Each gauge was mounted onto the PMMA substrate using a cyanoacrylate adhesive. A great care was taken to achieve the optimum precision regarding the location and the orientation of the gauges relative to the contact area. The actual positioning of the gauges with respect to the contact area was systematically measured from magnified pictures of the PMMA specimens after the tests. The measured values were used for all the calculations regarding the friction coefficient and the fretting loops (see below). The gauges were connected to a Philips MAS 010 conditioner (Cambridge, UK). The bridge was balanced after the contact normal loading in order to measure only the components of the surface strain induced by the tangential tractions.

2.2. Strain gauge arrangements

Friction induced strains on the surface of the PMMA have been measured by means of precision strain gauges. The size and the location of the gauges on the PMMA specimen were selected according to the following two considerations:

(i) the contact stress field is highly heterogeneous in nature and characterised by steep gradients close to the contact area. The active length of the gauges needs therefore to be minimised in order to limit the complications arising from the averaging of the strain gradients over a too large area. In addition, a compromise needs also to be found regarding the distance between the gauge and the contact zone; the gauge must be far enough from the contact to avoid the steep strain gradients, but also close enough to detect strains which are compatible with the gauge sensitivity. In the present study, a good compromise was obtained by using miniature strain gauges (grid length 1 mm) which were located between 3.5 and 5.5 mm from the centre of the contact area.

(ii) The contact loading generates a complex multiaxial stress field, while a gauge of the type selected can only measure the strain in a single direction. Under multiaxial loading, the usual route for the determination of the principal stresses components

is to use a classical 'rosette' arrangement, which involves the combination of at least three gauges oriented in different directions. Such a solution is, however, not easily practicable in the context of strain measurements in the vicinity of a contact, where the limited available space and the heterogeneous stress field would require the use of expensive and fragile miniature rosettes. From contact mechanics considerations, some simplified gauges arrangements can, however, be envisaged to measure the main strain component in the two extreme loading configurations, i.e. $\alpha = 0°$ and $\alpha = 90°$.

In the case of a twisting sphere on a flat ($\alpha = 0°$), Hetenyi et al. [14] and Hills et al. [15] have established that the interfacial shear stress, $\tau_{r\theta}$, is the only non-vanishing surface stress component induced by the tangential loading. Moreover, the stress distribution is rotationally symetrical, Fig. 2(a). $\tau_{r\theta}$ can thus be measured by mounting the gauges along the known direction of the principal stresses σ_1 and σ_2, which are oriented at $+/-45°$ from the radial direction. Four strain gauges arranged in a full Wheastone bridge configuration have been used in the arrangement depicted in Fig. 2(b). Two opposed gauges along the radial direction measure strains of equal magnitude and signs when the tangential loading is applied.

As it is shown below, the classical theory of Hamilton [16] for a sliding sphere on a semi-infinite half space can be used to assess the surface stress distribution under the linear sliding configuration ($\alpha = 90°$). This model shows that, outside the contact path and along the sliding direction, the tensile stresses $\sigma_{xx}(y = 0)$ and $\sigma_{yy}(y = 0)$ are principal stress components. Moreover, $\sigma_{yy}(y = 0)$ decreases much more rapidly than $\sigma_{xx}(y = 0)$ when the distance from the contact is increased. At about 4 mm from the contact zone, the calculated ratio $\sigma_{xx}(y = 0)/\sigma_{yy}(y = 0)$ is close to 10. Strain gauges oriented along the sliding direction can therefore be used to measure the main strain component $\varepsilon_{xx}(y = 0)$. If only the effects of the tangential tractions are considered, Hamilton's theory also demonstrates that tensile stresses of equal magnitudes and opposite signs are induced at two symmetrical locations with respect to the centre of the contact; Fig. 3(a). Provided that the gauges bridge is equilibrated after the normal loading, two strain gauges diametrically opposed with respect to the contact area (Fig. 3(b)) can therefore be used in a half-bridge configuration to measure ε_{xx}.

2.3. FEM simulations

FEM simulations were carried out in order to compute the surface strains under contact configurations where no analytical contact mechanics theories were available, i.e.

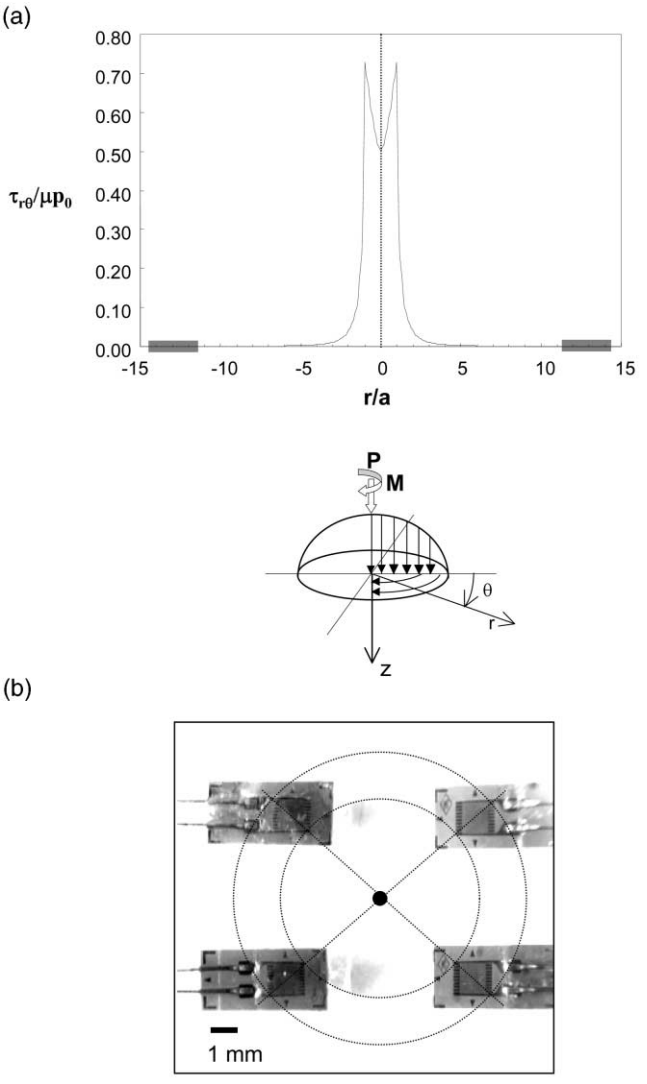

Fig. 2. Strain gauge arrangement on the surface of the PMMA for the measurement of $\gamma_{r\theta}$ under torsional contact conditions ($\alpha = 0°$). (a) Calculated distribution of the shear stress $\tau_{r\theta}$ generated along the r axis by the tangential loading (Eq. (7), p_0 is the maximum Hertzian pressure, μ is the coefficient of friction). The grey area indicates the gauge location. (b) Photograph of the four gauges oriented along the principal stress direction (the location of the contact area is indicated by a dark spot).

for $0 < \alpha < \pi/2$. 3-D computations were performed using a commercially available software package (SYSTUS+®, Systus International, France). The PMMA conterface was assumed to be linear elastic, while the steel sphere was approximated to a perfectly rigid body. The FEM software offered the possibility to simulate specified translational and rotational motions of the rigid ball, which were consistent with the requirements of the experimental configuration. Non-linear calculations were conducted using the mesh shown in Fig. 4 and a Coulomb's friction law at the contact interface. The normal indentation depth imposed to the steel ball (i.e. 10 μm) was numerically adjusted in order to reach the required

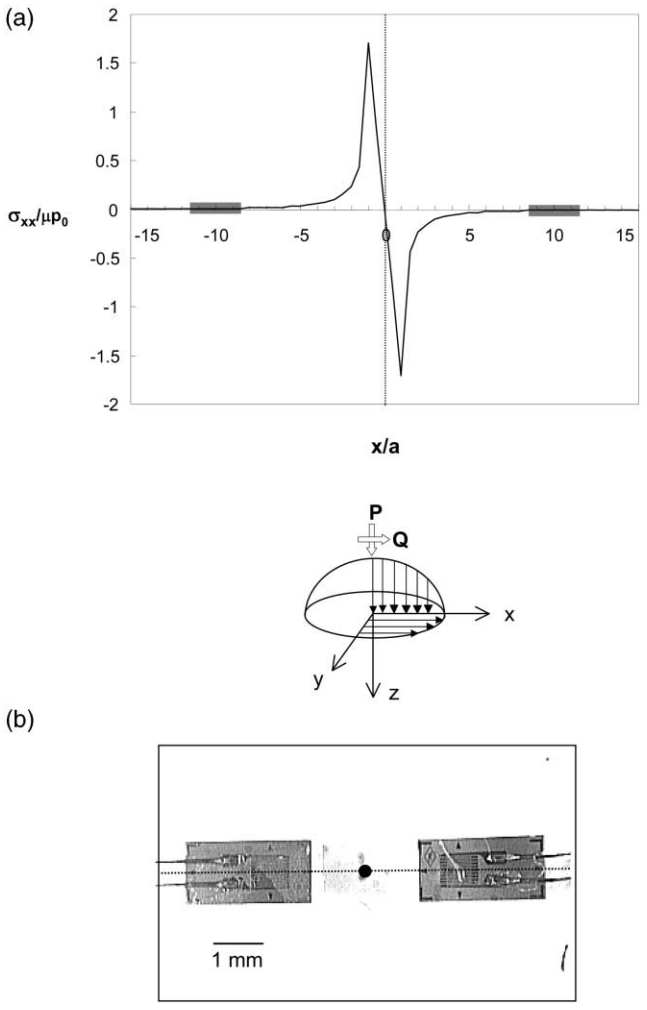

Fig. 3. Strain gauge arrangement on the surface of the PMMA for the measurement of ε_{xx} under linear sliding conditions ($\alpha = 90°$). (a) Calculated distribution of the axial stress σ_{xx} generated along the x axis by the tangential loading (Eq. (1), p_0 is the maximum Hertzian pressure, μ is the coefficient of friction). The grey area indicates the gauge location. (b) Photograph of the two gauges diametrically opposed with respect to the contact area (shown as a dark spot in the Figure).

value of the normal load (20 N). The axis of rotation of the steel ball was tilted at 0, 5, 10, 15, 30 and 90° with respect to a direction normal to the surface of the PMMA. The calculation provided the stress and strain field achieved under gross slip condition.

3. Results and discussion

3.1. Linear sliding conditions ($\alpha = 90°$)

Under fretting loading, the contact conditions are usually determined by plotting the tangential force as a function of the imposed displacement. By analogy, fretting loops giving the measured axial strain, ε_{xx}, as a function of the angular displacement of the steel ball are shown

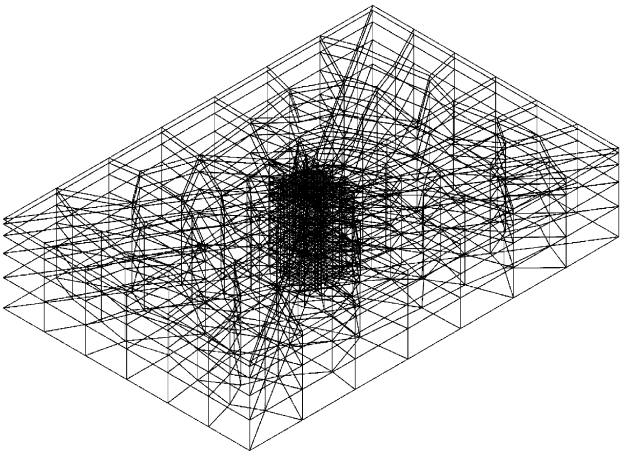

Fig. 4. 3D Meshing of the PMMA counterface for the FEM simulations of the surface strains.

in Fig. 5. At a low displacement amplitude, a linear behaviour is observed which indicates a predominantly elastic response of the system, with very limited microslip at the contact interface; Fig. 5(a). When the angle of twist exceeds a value of about 0.5°, a sharp transition to quasi-trapezoidal shaped fretting loops is observed; Fig. 5(c)–(e). In the plateau region of these loops, the constant surface strain can unambiguously be related to the achievement of a stationary stress field under gross slip condition. The strain gauge measurement therefore allows the accurate determination of the critical displacement amplitude at the transition from partial slip to gross slip, which is crucial for the analysis of the fretting induced damage.

The measured strain amplitude under gross slip condition can also be used to assess a value of the coefficient of friction. If Hamilton's theory for a sliding sphere is considered [16], the two principal stress components, σ_{xx} and σ_{yy}, along the x axis, can be expressed as follows:

$$\sigma_{xx} = \frac{3\mu P}{2\pi a^3} f(x,a) \qquad x > a \tag{1}$$

$$\sigma_{yy} = \frac{3\mu P}{2\pi a^3} g(x,a) \qquad x > a \tag{2}$$

Where P and μ are respectively the normal load and the coefficient of friction. $f(x, a)$ and $g(x, a)$ are two functions of the Poisson's ratio of the polymer, ν, the contact radius, a, and the distance x with respect to the centre of the contact:

$$f(x) = -x\left(1 + \frac{\nu}{4}\right) \tan^{-1}\left(\frac{a}{\sqrt{x^2 - a^2}}\right) + \frac{a\sqrt{x^2 - a^2}}{x^3}\left[x^2\left(\frac{5\nu}{4} + 1\right) - \frac{\nu a^2}{2}\right] \tag{3}$$

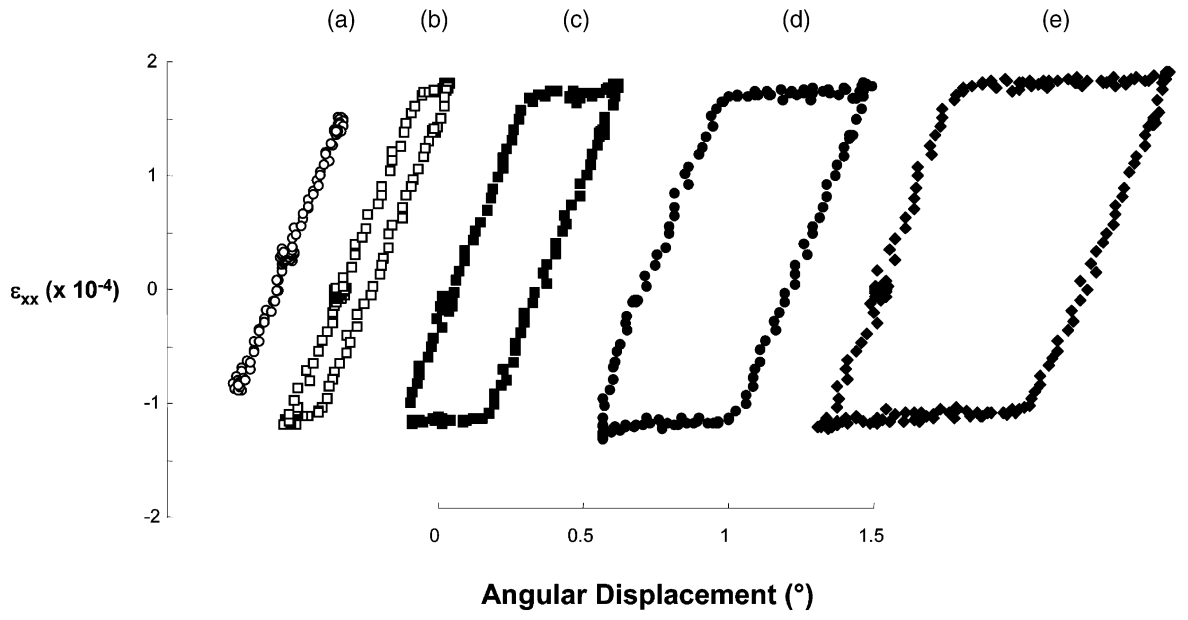

Fig. 5. Fretting loops obtained under linear sliding conditions ($\alpha = 90°$). (a) $\theta = 0.35°$, (b) $\theta = 0.55°$, (c) $\theta = 0.75°$, (d) $\theta = 0.9°$, (e) $\theta = 1.2°$.

$$g(x) = -\frac{3}{4}\nu x \tan^{-1}\left(\frac{a}{\sqrt{x^2-a^2}}\right) + a\frac{\sqrt{x^2-a^2}}{x^3}\left(\frac{\nu a^2}{2} + \frac{3}{4}\nu x^2\right) \quad (4)$$

Since the strain gauge bridge was balanced after the normal loading, only the stress components associated with the tangential loading were considered in Eqs. (1) and (2). Following Hooke's law, one can write:

$$\varepsilon_{xx} = \frac{1}{E}(\sigma_{xx} - \nu\sigma_{yy}) \quad (5)$$

With, E, the Young's modulus of the polymer counterface. By combining Eqs. (1), (2) and (5), the value of the coefficient of friction can thus be expressed as a function of the normal load, the measured strain ε_{xx} and the mean distance of the gauges with respect to the contact area:

$$\mu = \frac{2\pi a^3 E\varepsilon_{xx}}{3P(f(x) - \nu g(x))} \quad (6)$$

It is worth noticing that in expressions (1) and (2) the linear sliding is considered to result from the tangential displacement of a sphere on a semi-infinite flat. In the experimental situation, linear sliding is obtained in a slightly different manner, i.e. by the rotation of the rigid sphere about a stationary axis parallel to the surface of the flat. As a first approximation, it was assumed that the measured tensile strains were similar in both configurations. This hypothesis was verified by the numerical simulations which provided values of ε_{xx} very close to those given by Hamilton's theory: at the mean gauge location, i.e. $x = 3.5$mm, ε_{xx} was found to be equal to 1.0×10^{-4} and 1.05×10^{-4} for the FEM and the analytical model respectively (the value of the friction coefficient was taken as 0.5). Incidentally, the FEM simulations also demonstrated that the Hertzian pressure distribution remains largely unaffected by the tangential loading associated to the torsion of the sphere (Fig. 6), which is one of the basic assumption of the Hamilton's approach. Accordingly the stresses induced by the tangential and normal loading can be considered as decoupled, as it is implicitly assumed in Eqs. (1) and (2).

On the basis that Hamilton theory is applicable in the context of the current experiments, the coefficient of

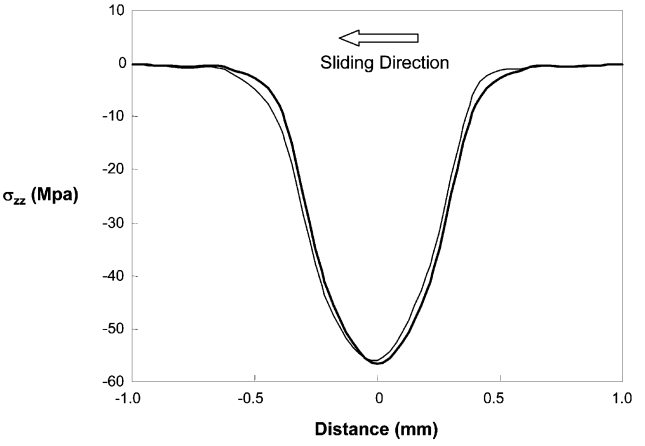

Fig. 6. FEM simulation of the distribution of the normal pressure under a combined normal and tangential loading ($\alpha = 90°$). Bold line: normal loading only; sharp line: normal and tangential loading.

friction was subsequently calculated using Eq. (6) by incorporating the measured value of the strain amplitude under gross slip conditions ($\varepsilon_{xx} = 1.5 \times 10^{-4}$). For an improved accuracy, the functions $f(x)$ and $g(x)$ have been averaged over the distance covered by the active length of the gauge. A mean value of 0.73 was computed for μ, which is consistent with the data reported in the literature for similar systems under fretting conditions [17].

3.2. Torsional contact conditions

Fretting loops giving the surface shear strain $\tau_{r\theta}$ as a function of the angle of twist, θ, are shown in Fig. 7. For the lowest displacement amplitude (i.e. θ less than 2°), quasi-elliptical fretting loops were obtained. This non-linear behaviour is characteristic of the progressive development of micro-slip from the periphery of the contact towards the centre of the contact [18]. As the magnitude of the angle of twist is increased, the occurrence of the gross slip conditions is indicated by the plateau value of the surface shear strain. It can also be noted that the measured strains are much lower than those recorded under the linear sliding configuration.

As for the case of linear sliding conditions, a calculation of the coefficient of friction from the measured shear strain amplitude under gross slip condition can be implemented by means of contact mechanical procedures. The theoretical expressions for the surface stresses induced by a twisting sphere were initially derived by Hetenyi et al. [14] in an early paper. This calculation, however, required the difficult numerical integration of the oscillatory Bessel functions. To overcome this problem, Hills et al. [15] have developed an alternate scheme involving elliptic integrals. According to this approach, the surface shear stress, $\tau_{r\theta}$ is given by the following expression:

$$\frac{\tau_{r\theta}}{\mu p_0} = \frac{2}{\pi r^2}\int_0^1 \frac{t^2 E(t')\mathrm{d}t}{\sqrt{r^2 - t^2}} \tag{7}$$

where $t' = \sqrt{1-t^2}$, $E(x)$ is the complete elliptic integral of the second kind and r is the space coordinate non-dimensionalised with respect to the contact radius, a. p_0 is the maximum Hertzian pressure defined as:

$$p_0 = \frac{3P}{2\pi a^2} \tag{8}$$

Assuming a linear elastic behaviour for the PMMA, the value of μ is thus given by:

$$\mu = \frac{\pi r^2 G \gamma_{r\theta}}{2p_0 \int_0^1 \frac{t^2 E(t')\mathrm{d}t}{\sqrt{r^2 - t^2}}} \tag{9}$$

Expression (9) can readily be numerically integrated, thus providing a value of μ from the measurement of $\gamma_{r\theta}$. A mean value of 0.67 was found, which is similar to those obtained under linear sliding conditions, μ=0.73. This constancy of μ for the different gauge arrangements and loading configurations confirms the overall consistency and the accuracy of friction measurements from surface strains.

From the knowledge of the friction coefficient, a further attempt was made to simulate a whole fretting loop. In addition to Eq. (9) for gross slip condition, this calculation requires a knowledge of the surface strain induced under partial slip condition. Although the theory

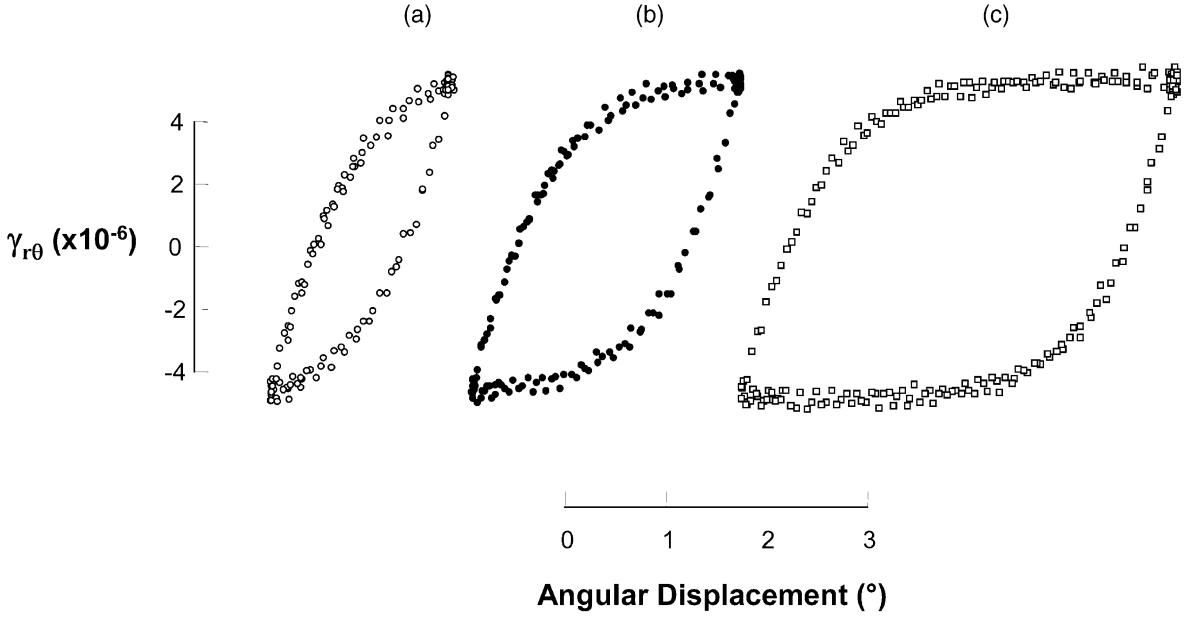

Fig. 7. Fretting loops obtained under torsional contact conditions ($\alpha = 0°$). (a) $\theta = 1.8°$, (b) $\theta = 2.2°$, (c) $\theta = 4.2°$.

does not provide any direct relationships between the shear strain and the angle of twist under partial slip condition, both $\gamma_{r\theta}$ and θ can be related independently to the radius, c, of the stick/slip boundary within the contact ($0 < c < a$). $\gamma_{r\theta}$ is given by [15]:

$$\gamma_{r\theta} = \frac{2\mu p_0}{3G\pi}\frac{k}{rc}[2(c^2-r^2)K(c/r) + (2r^2-c^2)E(c/r)] \quad (10)$$

$$-\frac{2\mu p_0}{\pi G r^2}\int_0^c \frac{t^2}{\sqrt{r^2-t^2}}[E(\eta,t') + E(\chi,t')]\mathrm{d}t \qquad r >= c$$

with:

$$k^2 = 1-c^2$$

$$\sin\chi = \frac{1}{c}\sqrt{\frac{c^2-t^2}{1-t^2}}$$

$$\sin\eta = \frac{k}{t'}$$

while the expression of the angle of twist, θ, as a function of c is given by [18]:

$$\theta = \frac{3\mu P}{4\pi G a^2}k^2 D(k) \quad (11)$$

with $D(k) = (K(k) - E(k))/k^2$, where K and E are, respectively, the complete elliptic integrals of the first and second kind, of modulus k.

By evaluating separately Eq. (10) and (11) for different values of c ranging from 0 to 1, it is possible to generate a complete set of (θ, $\gamma_{r\theta}$) values corresponding to various extents of partial slip and thus to simulate a whole fretting loop. An example using the experimental value of the coefficient of friction is shown in Fig. 8. The good agreement observed between the experimental and theoretical values constitutes, to the best of our knowledge, the first experimental validation of the theoretical expressions for the surface stresses beneath a twisting sphere under partial slip conditions (the equations for gross slip conditions have already been validated by Hetenyi et al. by means of the examination of a set of very carefully generated photo-elastic measurements).

3.3. Intermediate contact loading configurations

When the angle of tilt, α, (Fig. 1a) is increased from 0° (torsional contact loading) to 90° (linear sliding configuration), a complex stress state is achieved which can no longer be satisfactorily described by the available analytical contact mechanics theories. As was mentioned above, a complete determination of the surface stresses would require a set of strain gauges arranged in a delicate 'rosette' configuration. In a previous investigation [13], we have, however, reported that the linear motion condition rapidly dominated the sliding trajectories as the contact loading was varied from pure torsion to pure linear sliding; for values of $\alpha > 5°$. This argument was based upon purely geometrical considerations, with no attempt to describe the contact conditions from a mechanical point of view. A more detailed insight of the contact conditions can be provided by F.E.M. calculations. In Fig. 9, the calculated profiles for ε_{xx} in the contact zone are reported as a function of α. It can be seen that the ε_{xx} distribution becomes identical to that achieved for linear sliding motion when α exceeds 5°. This result was experimentally confirmed by the measurements of the axial strain, ε_{xx}, as a function of the tilt angle. Using the same gauge arrangement as for the $\alpha = 90°$ configuration, it was observed (Fig. 10) that ε_{xx} reaches very rapidly the value achieved under pure linear sliding as the tilt angle is increased.

In the processing of the output signal coming from the Wheastone bridge, we have considered that the two opposite active gauges were measuring stresses of equal magnitude, but opposite signs, whatever the angle of tilt;

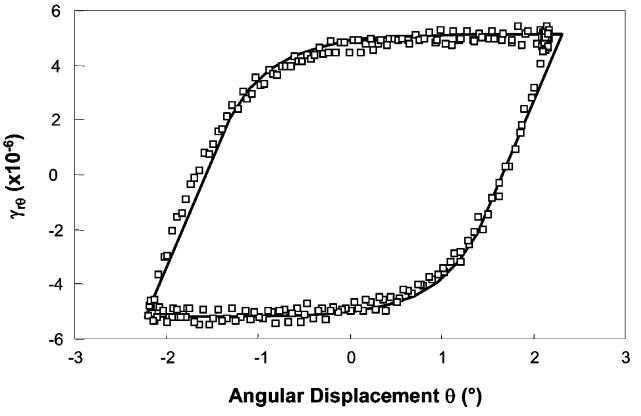

Fig. 8. Simulated and experimental fretting loop under torsional contact conditions ($\alpha = 0°$). (The theoretical loop was calculated using Eqs. (7), (10) and (11) with $\mu = 0.7$).

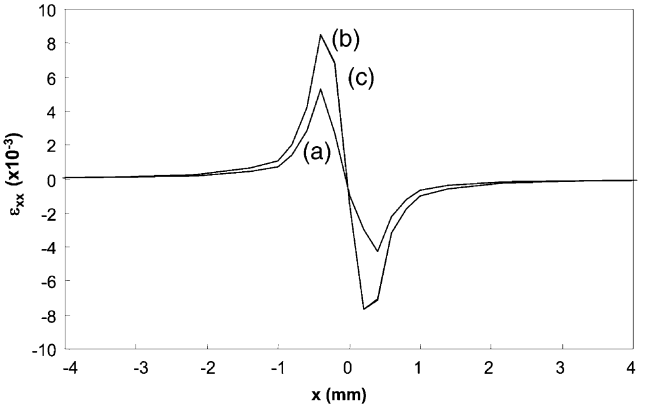

Fig. 9. Calculated (FEM) profiles of ε_{xx} as a function of the tilt angle α. (a) ($\alpha = 5°$), (b) ($\alpha = 10°$), (c) $\alpha = 90°$; curves (b) and (c) are superimposed; $\mu = 0.5$.

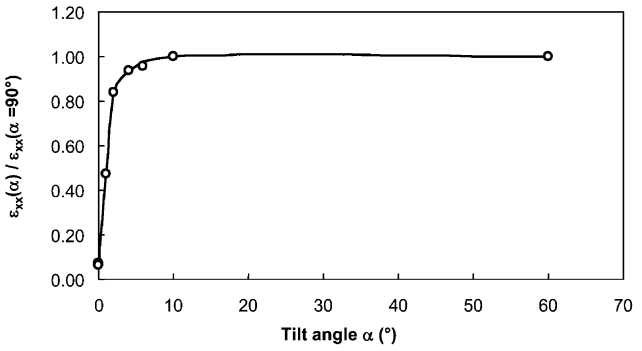

Fig. 10. Changes in the experimental values of the axial surface strain ε_{xx} as a function of the tilt angle,α. The strain value have been normalised with respect to the ε_{xx} value for $\alpha = 90°$. For $\alpha > 5°$, though linear motions predominates within the contact.

Table I shows this hypothesis to be reasonably valid based upon FEM simulations.

4. Conclusion

A novel technique based upon experiments, analysis and numerical simulations has been proposed in order to determine the contact conditions and the values of the friction coefficient in contacts submitted to various loading conditions including torsion and linear sliding motions. In the case of a low modulus polymeric substrate (PMMA), it was demonstrated that strain gauge measurements of the friction induced surface strains allowed an accurate estimate of both the friction coefficient and the contact conditions generated under small amplitude oscillating micro-motions (fretting). The overall potential of the method was supported by the constancy of the calculated values of the friction coefficient under the various contact loading configurations considered. The measurements also provided the first experimental confirmation of some of the theoretical results regarding the stress field induced by a twisting sphere in a semi-infinite medium.

The strain gauge measurements have also demonstrated the ability to detect the changes in the surface stress state when a varying multiaxial contact loading was considered, i.e. in a situation where conventional load transducer based measurements of the friction forces are not easily performed. In the case of contact conditions induced by low amplitude sliding micromotions (fretting), it was also shown that the surface strain measurements allowed an accurate description of the transition from stick to slip condition as the magnitude of the imposed displacement was increased. This transition is of major importance in fretting studies due to the fact that it governs the nature of the induced surface damage. In the current experiments, it was determined without the difficulties arising from the use of compliant load transducers.

By virtue of the reduced spatial hindrance of the gauges, such a technique presents the advantage of being able to be operated with a great flexibility in a wide range of contact configurations. The determination of the absolute value of the friction coefficient relies upon the use of elastic contact mechanics theories, which are derived for semi-infinite medium and for relatively simple contact configurations. If it is assumed that the magnitude of the surface induced strains remains proportional to the friction coefficient, this technique could, however, still be used to monitor relative changes in μ in the case of thin substrates or for more complex contact geometries.

Table 1
Calculated axial strain, ε_{xx}, at two locations diametrically opposed with respect to the contact area

	x=-L	x=+L
$\alpha = 0°$	0.01	0.02
$\alpha = 5°$	0.68	0.65
$\alpha = 10°$	1.02	0.99
$\alpha = 15°$	1.02	0.99
$\alpha = 90°$	1.00	1.00

Gross slip condition, $\mu = 0.5$, L is the mean distance of the strain gauge location with respect to the centre of the contact, ε_{xx} was non-dimentionalised with respect to the value for $\alpha = 90°$

Acknowledgements

The authors fully acknowledge the financial support of the Royal Society (UK) and Centre National de la Recherche Scientifique (France). Many thanks are also due to Marie Chaze (Laboratoire de Tribologie et Dynamique des Systèmes, Lyon, France) for her technical assistance in the FEM simulations.

References

[1] Dowson D. The history of tribology. London: Professional Engineering Publishing, 1977.
[2] Eldredge KR, Tabor D. Proc Roy Soc London, Ser A 1955;229:181.
[3] Bowden FP, Leben L. Proc Roy Soc London, Ser A 1939;169:371.
[4] Bristow JR. Proc Roy Soc London, Ser B 1950;53:964.
[5] Hirst W, Kerridge M, Lancaster JK. Proc Roy Soc London, Ser A 1952;212:516.
[6] Adams MJ, Briscoe BJ, Kremnitzer SL. A survey of the adhesion, friction and lubrification of polyethylene terephthalate monofilaments. In: Mittal KL, editor. Physicochemical aspects of polymer surfaces. New York: Plenum Press; 1983. p. 425–50.
[7] Briscoe BJ, Kremnitzer SL. A study of the friction and adhesion of polyethylene-terephthalate monofilaments. J Phys D 1979;12:505–16.

[8] Fouvry S, Kapsa P, Vincent L. Quantification of fretting damage. Wear 1996;200(1-2):186–205.
[9] Johnson K. Surface interaction between elastically loaded bodies under tangential forces. Proc Roy Soc London, Ser A 1955;230:531–48.
[10] Mindlin RD. Compliance of elastic bodies in contact. Trans ASME Ser E J Appl Mech 1953;16:327–44.
[11] Vincent L. Materials and fretting. Fretting fatigue ESIS 18. London: Mechanical Engineering Publications, 1994 p. 323-337.
[12] Briscoe BJ, Chateauminois A, Lindley TC, Parsonage D. Fretting wear behaviour of PMMA under linear motions and torsional contact conditions. Tribology Int 1998;31(11):701–11.
[13] Briscoe BJ, Chateauminois A, Parsonage D, Lindley TC. Contact damage of poly(methylmethacrylate) during complex micro-displacements. Wear 2000;240:27–39.
[14] Hetenyi M, McDonald PH. Contact stresses under combined pressure and twist. Trans ASME 1958;25:396–401.
[15] Hills DA, Sackfield A. The stress field induced by a twisting sphere. Trans ASME J Appl Mech 1986;53:372–8.
[16] Hamilton GM. Explicit equations for the stresses beneath a sliding spherical contact. Proc Inst Mech Eng 1983;197C:53–9.
[17] Dahmani N, Vincent L, Vannes B, Berthier Y, Godet M. Velocity accommodation in polymer fretting. Wear 1992;158(1-2):15–27.
[18] Deresiewicz H. Contact of elastic spheres under an oscillating torsional couple. Trans ASME J Appl Mech 1954;21:52–6.